

Article

Optimization of Aggregate Production Circuit through Modeling of Crusher Operation

Tomasz Gawenda  and Daniel Saramak * 

Department of Environmental Engineering, Faculty of Civil Engineering and Resource Management, AGH University of Science and Technology, 30-059 Cracow, Poland; gawenda@agh.edu.pl

* Correspondence: dsaramak@agh.edu.pl

Abstract: The paper concerns investigation of the effect of impact crusher operation on selected qualitative characteristics of mineral aggregate products. Qualitative characteristics of crushing products in terms of size reduction ratio and fine particles contents were analyzed from the point of view of operational parameters of the impact crusher. An investigative program was carried out on a plant scale and two primary parameters of the impactor were analyzed: velocity of the crusher rotor and the width of the outlet gap. The models of the crushing device operation were built separately for each type of the tested material, as well as for general conditions.

Keywords: aggregate; mineral processing; comminution; particle size; particle shape



Citation: Gawenda, T.; Saramak, D. Optimization of Aggregate Production Circuit through Modeling of Crusher Operation. *Minerals* **2022**, *12*, 78. <https://doi.org/10.3390/min12010078>

Academic Editors: Chiharu Tokoro, Ngonidzashe Chimwani and Murray M. Bwalya

Received: 6 November 2021

Accepted: 7 January 2022

Published: 9 January 2022

Publisher's Note: MDPI stays neutral with regard to jurisdictional claims in published maps and institutional affiliations.



Copyright: © 2022 by the authors. Licensee MDPI, Basel, Switzerland. This article is an open access article distributed under the terms and conditions of the Creative Commons Attribution (CC BY) license (<https://creativecommons.org/licenses/by/4.0/>).

1. Introduction

Production of mineral aggregates is realized in processing circuits that use mostly crushing and screening operations. However, these relatively simple systems require a certain control and need to be adopted to the characteristics of the feed material as well as to expected technological outcomes [1]. Three main groups of variables can be distinguished when an issue of improvement of work effectiveness is considered:

- Physical and mechanical parameters of the feed material,
- Operational parameters of crushing and screening devices,
- Parameters linked with the type of technological process or operation.

Properties of the feed material seem to be of crucial impact on the quality of obtained products, especially in terms of strength characteristics of specific fractions of aggregates or quality of produced concrete and asphalt mixtures [2–4]. The shape of particles also affects the outcomes of some operations of mechanical processing, like gravity concentration and hydraulic classification [5,6]. Particles that are irregular in shape, i.e., elongated, oblong, or flat, are undesired in final products, and qualitative requirements and standards determine maximum boundary contents of such particles [7].

Results of investigations show that depending on the type of rock material, there can be usually observed a correlation between the content of irregular particles in feed and in products [1,2], and when the yield of irregular particles in feed is significant, it is relatively harder to obtain products with regular particles. The technological regime, process course, and especially the type of applied crushing devices have a great impact on the shape of obtained products [8–12]. There can be observed various ideas and solutions aiming at irregular particles in the crushing products, both in crushing and screening operations. Several patents were worked out as well [13]. Scanning techniques utilizing image analysis vision systems are also helpful in accurate characterization of the granular material properties and usually help in real-time process control [14,15].

The crushing process is of key significance in the aggregate processing sector but is also of a special concern in raw materials treatment, in general. In ore processing it applies both crushing and grinding operations, for the reason they are energy consuming,

and breakage effectiveness is relatively low, especially in grinding operations in tumble mills [16]. Industrial comminution consumes from 3 to 5% of world electric energy usage [17], and negatively affects the environment through high rates of CO₂ emission, as well as noise, dust, and heat generation [18–23]. It leads to deterioration of the living standards of inhabitants in the vicinity of mineral processing plants and constitutes a potential health risk for mine workers [24].

2. Problem Significance and Research Motivation

Results of up-to-date investigations as well as an industrial practice show that crushing and classifying circuits, despite their relative simplicity, may operate with too low effectiveness, in terms of insufficient size reduction ratio, lower liberation level (in case of ores), or inaccurate particle size distribution of final products. Most frequently, the type and general strength properties of the feed are taken into consideration at the starting point of the optimization approach. However, results of various investigations show that particle shape of aggregate product [25,26] significantly influences the qualitative characteristics of concrete mixes and cement mortars with adding of such aggregate. It is, however, worth mentioning that the problem of control the crushing products characteristics—is the subject of many studies. It is common to all types of granular materials: from coals [27], through aggregates and cement powder production, ending on ore processing, and relates both to crushing and grinding devices. More investigative programs were carried out for crushing devices, due to relatively higher number of operational parameters (i.e., gap, frequency of rotation, jump, profile of liners, nip angle, and others), and higher potentials of their steering [28]. The models worked out for crushing devices that usually operate on entire crushing stages, like cone and jaw crushers, were developed in works of Whiten [29,30] where the breakage function was described as a functional relationship of the feed particle size distribution. More recent investigations focus on impact crushers, where the authors have taken into consideration both the operational parameters of crushing devices and feed characteristics. In Ref. [31], the model based on classification and breakage matrices that depended both on the rotor radius, angular velocity, and the throughput was developed. The Weibull's distribution was used in modeling and the results were compared with data achieved in plant-scale operation. Models of size distribution for products from various crushers were developed in [32,33], where statistical distribution of t-family was used, and material characteristics based on Bond index values were taken into consideration. Investigations were carried out for limestone samples and a high value of determination coefficient was achieved.

An approach aiming at improvements of aggregate production effectiveness should also focus on the final effects that are achieved as an operation of the entire circuit, not only a single device. It means that a key-device should be optimized, but the potential effect should be related to qualitative parameters of the final products, not only to the crusher product. The scope of the presented paper investigates an impact of the crusher device operation on the production of the fine aggregates. A practical tool for control (model) was developed, and showed what effects could be expected, for specific values of primary operational parameters of the crusher. The two main parameters were used in the model and the influence of each of them was determined, so it was possible to observe which parameter has a potentially greater impact on the final effect. Such a model can be developed, and a higher number of values can be used, depending on the requirements and specific situation. It is worth remembering that heuristic analysis should be performed prior to modeling. The presented approach is a novelty, and not commonly met in literature.

3. Materials and Methodology

3.1. Circuit and Device Characteristics

An investigative program was carried out on an industrial scale on an aggregate production circuit operating in the *Dolomite Imielin Mine*, located in Imielin, in Silesia

(Poland). The mine extract rock raw materials in an open pit system and also operates circuits of mineral aggregate production.

The circuit that was the object of investigations consisted of two-stage crushing processes and a series of screening and sieve classification operations. The product from a first stage of crushing in the jaw crusher is downstream classified in a three-decked vibrating screen. The size fraction over 120 mm is re-crushed in the impactor, products of which are subjected to further classification, as a result of what the further fine sized fractions of products can be obtained. A simplified scheme of the circuit is presented in Figure 1.

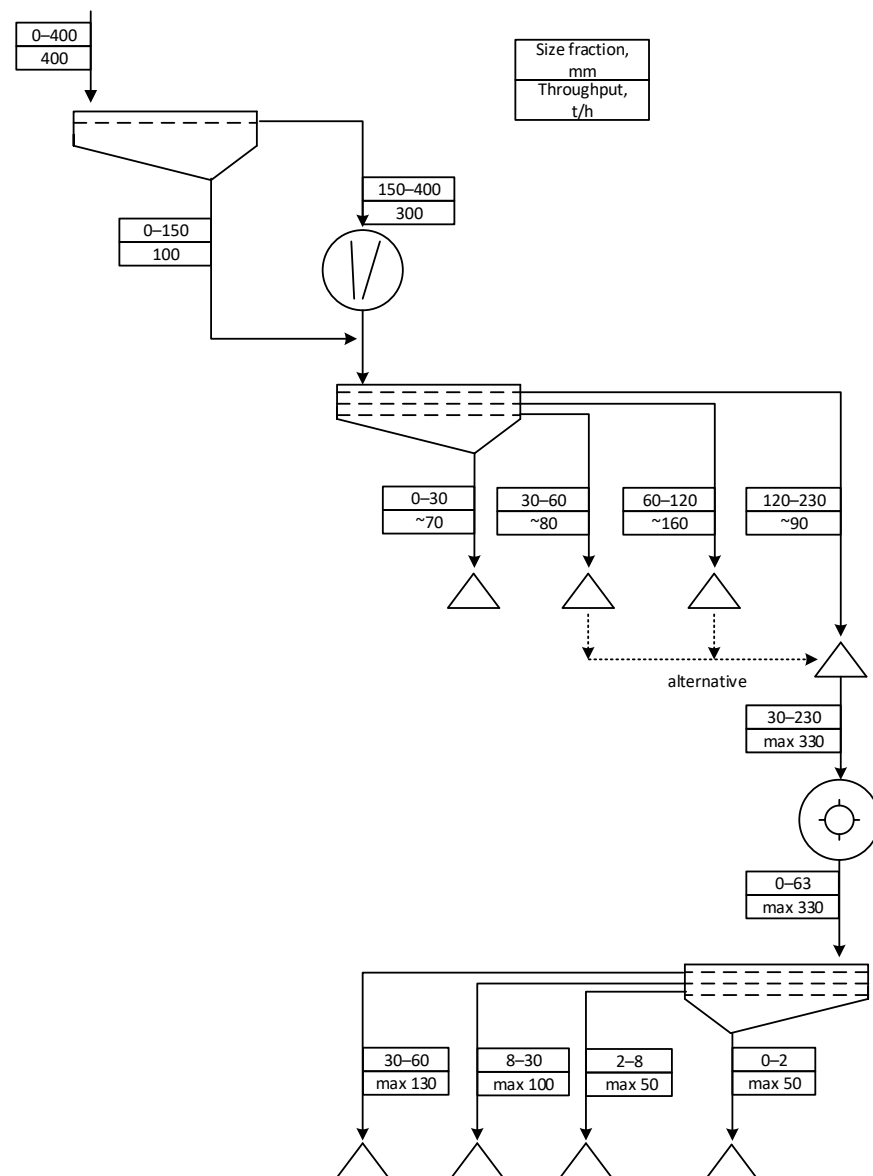


Figure 1. Technological circuit under testing.

The main purpose of the investigations is an assessment operation of an impact crusher that operates on the second crushing stage. This is a device of key significance in the circuit, because its crushing product is classified into final products according to specific particle size fractions (see Figure 1), and at the same time constitutes the final aggregate products. This type of crushing device is quite commonly used in aggregate production circuits due to the fact that crushing products contain relatively lower content of irregular (i.e., flat, elongated) particles comparing to jaw crushers, what is often expected for aggregate products.

The tested impact crusher KU65-120 (Figure 2a) is the device with horizontal shaft, equipped with four blades, and powered by a 200 KW engine. Dimensions of an inlet of the working chamber are 650 mm × 1200 mm. Three consecutive gaps are in the working chamber of the crusher and each of them is adjustable, according to requirements. The last one, called the calibrating gap (Figure 2b), has the smallest width, which was subject to change in the investigative program. The first and the second gaps remained constant during experimental program and equaled 20 and 90 mm, respectively. The speed of rotor is controlled by adjustment of a specific frequency value on the thyristor box. For example, the frequency within the range 40–50 Hz corresponds to rotor velocity from 30 to 38 m/s.



Figure 2. Crushing device—impact crusher KU 65-120 during investigations (a); calibrating gap in the crusher (b).

The rotational speed of the rotor was the other operational changeable parameter. Nominal throughput of the crusher varies from 200 to 300 Mg/h depending on the breakage resistance of the crushed material. The machine is equipped with a counter of the power consumed during operation. This value was registered during the testing program and the unit energy consumption was calculated as a relationship of total power consumed to the throughput of the machine.

The device is top-fed by means of vibrating feeder. The material entering the working chamber is subjected to a series of collisions with the rotating blades of the rotor, walls and plates of the chamber, as well as other particles and after that exits the chamber as suitably finer particles, and around 80% of them have a regular shape.

3.2. Material Properties

Five types of feed material were used in the testing program: dolomite (M1), limestone (M2), gravel (M3), sandstone (M4), and diabase (M5). Maximum particle size of gravel feed was 150 mm, while dolomite and limestone D_{max} equaled 200 mm. Maximum size of diabase was 250 mm and the coarsest material, sandstone, was characterized with maximum particle size 300 mm. Detailed characteristics of particle size distributions of individual material types in semi-log scale are presented in Figure 3.

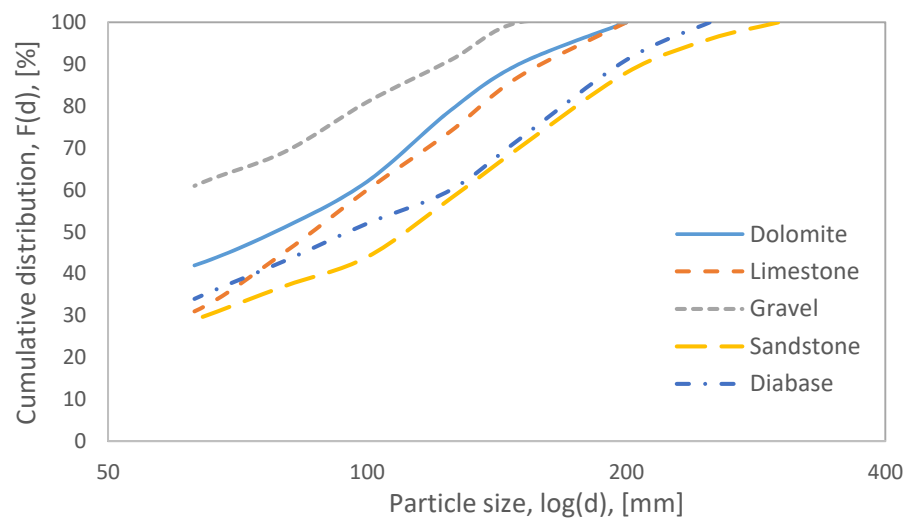


Figure 3. Particle size distributions of all types of material used in investigations.

Particle size distributions of individual types of materials differ, which is due to various conditions, i.e., internal structure of material, physical and mechanical properties of the feed, upstream mining techniques of material treatment, including blasting and primary crushing. Therefore, comparative analysis was based on achieved size reduction ratios S_{90} . Limestone and sandstone can be characterized as materials that are easily crushed, while diabase and gravel showed the highest breakage resistance. Values of Bond's work indices (BW_i) were determined that equal, respectively, for the sandstone $BW_i = 9.2$ kWh/t, for limestone $BW_i = 9.9$ kWh/t, for dolomite $BW_i = 11.6$ kWh/t, for gravel $BW_i = 13.1$ kWh/t, and for diabase $BW_i = 13.4$ kWh/t. The values were determined according to the Bond's procedure in laboratory ball mill with dimensions 305 mm × 305 mm. The material volume for each single batch test was 700 cm³ with the load of 285 steel grinders (balls) (20.1 kg) with diameters from 15.2 to 38.1 mm.

Investigations were carried out on an industrial scale. The parameters of the device were set accordingly, and the production started. Samples of specific crushing products in a total mass about 200 kg each, were collected from the belt, after stabilization of the circuit capacity. Next, they were subjected to a mass reduction with use of a riffle sample splitter. Mass of a single sample for further analyses amounted from 30 to 50 kg, depending on the particle size of individual crushing products. After the sample collection, the settings of operational parameters were changed according to the testing program and after further stabilization of the circuit operation, another sample was collected.

3.3. Structure of the Model

Tests for various types of material and various operational parameters of the crusher were included in an investigative program. The variables can be therefore grouped into two categories: the one connected with material properties, and the other related to characteristic of the crushing device. A general form of the mathematical model can be written as follows:

$$y = f(\text{material type, rotor velocity, gap}) \quad (1)$$

where y denotes a dependent value, which was defined either as a size reduction ratio S_x , or as yield of the finest product (FPI). The size reduction ratio, presented in Formula (2), is an index calculated as a relation of characteristic particle in the feed (i.e., D_{50}, D_{80}, D_{90}) to the characteristic particle of the product (i.e., d_{50}, d_{80}, d_{90}).

$$S_x = \frac{D_x}{d_x} \quad (2)$$

The second dependent variable, *FP1*, was obtained during the sieve analysis performed for each crushing product. The *FP1* denotes yield of the finest particle size fractions, i.e., below 2 mm, that existed in individual crushing product. Feed analysis shows (Figure 3) that none of the material contains size fractions below 2 mm. Determined values of both dependent variables for each crushing products are presented in specific columns in Tables 1–6, along with the other results of experiments.

Table 1. Scheme of the investigative program.

Number of Sample	Variable 1 (Velocity)	Variable 2 (Gap)	M1	M2	M3	M4	M5
I	30	40	Yes	Yes	Yes	Yes	Yes
II	34	40	Yes	Yes	Yes	No	No
III	38	40	Yes	Yes	Yes	Yes	Yes
IV	30	60	Yes	Yes	Yes	No	No
V	34	60	Yes	Yes	Yes	No	No
VI	38	60	Yes	Yes	Yes	No	No
VII	30	80	Yes	Yes	Yes	Yes	Yes
VIII	34	80	Yes	Yes	Yes	No	No
IX	38	80	Yes	Yes	Yes	Yes	Yes

Table 2. Results obtained for dolomite (M1).

Sample Number	Speed of Rotor	Gap	<i>Q</i>	<i>Esp</i>	<i>FP1</i>	<i>S</i> ₉₀
1	30	40	262	0.27	11.0	5.4
2	34	40	255	0.32	12.5	5.8
3	38	40	250	0.46	14.9	6.2
4	30	60	267	0.30	9.3	3.9
5	34	60	258	0.33	13.1	3.9
6	38	60	254	0.47	12.4	4.5
7	30	80	286	0.30	10.0	3.6
8	34	80	275	0.34	10.1	3.8
9	38	80	263	0.48	12.2	3.2

Table 3. Results obtained for limestone (M2).

Sample Number	Speed of Rotor	Gap	<i>Q</i>	<i>Esp</i>	<i>FP1</i>	<i>S</i> ₉₀
1	30	40	273	0.26	13.6	4.6
2	34	40	264	0.33	13.8	6.1
3	38	40	253	0.47	18.2	7.0
4	30	60	277	0.29	12.3	4.3
5	34	60	268	0.33	14.5	4.2
6	38	60	254	0.49	16.4	4.9
7	30	80	294	0.30	7.1	4.0
8	34	80	283	0.32	10.3	4.1
9	38	80	270	0.47	14.3	4.3

Table 4. Results obtained for gravel (M3).

Sample Number	Speed of Rotor	Gap	<i>Q</i>	<i>Esp</i>	<i>FP1</i>	<i>S</i> ₉₀
1	30	40	165	0.38	16.4	4.4
2	34	40	155	0.43	17.5	5.3
3	38	40	142	0.54	20.3	6.1
4	30	60	178	0.40	12.8	3.5
5	34	60	169	0.46	13.5	3.4
6	38	60	151	0.55	16.5	3.6
7	30	80	230	0.41	9.1	2.6
8	34	80	210	0.50	13.2	3.1
9	38	80	201	0.57	15.4	3.4

Table 5. Results obtained for the sandstone (M4).

Sample Number	Speed of Rotor	Gap	Q	Esp	FP1	S ₉₀
1	30	40	283	0.33	12.2	6.4
2	38	40	261	0.53	16.8	7.4
3	30	80	297	0.40	8.1	4.0
4	38	80	284	0.53	11.4	4.5

Table 6. Results obtained for the diabase (M5).

Sample Number	Speed of Rotor	Gap	Q	Esp	FP1	S ₉₀
1	30	40	253	0.39	10.1	5.1
2	38	40	241	0.60	13.8	5.7
3	30	80	271	0.46	7.1	3.7
4	38	80	256	0.64	9.4	4.0

The experimental program was conducted according to methodology of factorial experiments [34,35], in which various levels of variability were used, depending on the type of variable. Two major operational parameters of the impact crusher (variable 1 and variable 2) were selected as independent variables in specific models and three levels of changeability were assumed for each of them.

For variable 1 (linear velocity of rotor) values 30, 34, and 38 m/s were tested, while for the gap (variable 2) the widths 40, 60, and 80 mm, were used. During the crushing process two additional operational parameters were registered:

- Crusher's productivity, Q ,
- Unit energy consumption, E_{sp} .

In the case when each testing variable has the same number of changeability levels, the total number of required single experiments to be performed can be described through Formula (3).

$$N = n^k \quad (3)$$

where k —number of variables; n —number of variability levels. For the above assumptions nine single experiments were carried out for a given type of feed material. Investigations were carried out for five various types of feed materials, in order to check the potential effect of material on crushing results. The material type can be then treated as a variable 3, with five levels of changeability.

A complete factorial experiment was conducted for materials M1, M2, and M3, with $N = 9$ tests for each material. On the basis of the obtained results, it was possible to reduce the one variability level for the variable v_1 (34 m/s of rotor's linear velocity) in the testing of materials M4 and M5. The results indicated that it was also possible to eliminate the middle value of variable v_2 (gap 60 mm), and the further tests, conducted on materials M4 and M5, included two variables with two levels of changeability. A factorial experiment with $N = 4$ tests was conducted for materials M4 and M5. A detailed testing scheme is presented in Table 1.

As it was defined in Formula (1), for each configuration of independent variables, the crusher's work models were calculated separately for $FP1$ and S_{90} .

Considering the above, the Formula (1) can be written as follows:

$$Y(FP1, S_{90}) = f(\text{speed of rotor, gap}) \quad (4)$$

where: $FP1$ —yield of the finest product; S_{90} —90% size reduction ratio. In total, 35 single experiments were conducted on plant scale.

4. Results

Tables 2–4 present the achieved results for materials M1–M3: dolomite, limestone, and gravel, respectively.

Analysis of throughput (Figure 4) shows that the highest diversity in results can be observed for the material M3 (gravel) and the lowest for dolomite (M1). However, changeability for limestone (M2) was almost identical as for dolomite. The results obtained for material M3 were also the lowest in absolute numbers. It can be stated that processing of broken aggregates (M1 and M2) can be carried out at higher throughputs, while for the gravel much less favorable throughput was achieved. This is due to physical properties of the material and individual characteristics related to breakage resistance. It is not possible to clearly state which of the variables have a more significant impact on the throughput, especially for broken aggregates, i.e., materials M1 and M2. It is, however, visible that the gap width is proportionally correlated with the productivity, while the speed of rotor shows an inverse relationship: an increase in the speed of rotor from 30 to 38 m/s is effective in decreasing the throughput value by nearly 10%. This is due to the higher number of collisions with the rotor and plates, that a single particle experiences in the working chamber. The relationship between speed of rotor and the throughput for the gravel material is similar to materials M1 and M2, also in terms of the magnitude of changeability, but the gap has a significantly higher impact on the throughput. Increasing the gap from 40 to 80 mm causes the throughput increase by about 30%.

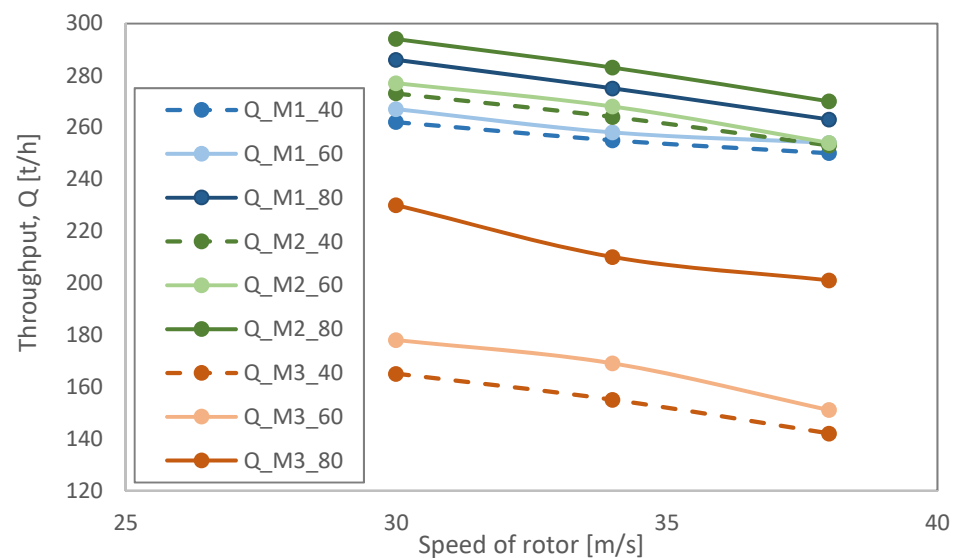


Figure 4. Results of throughput for various speeds of the rotor for materials M1–M3.

Both the relationship between a unit energy consumption and the speed of rotor appear to be proportional for all tests (Figure 5). For materials M1 and M2, an increase in the E_{sp} together with the higher values of the speed of the rotor is more intense than for the gravel—Figure 4. On the basis of these results, it can be stated that in the case of broken aggregates the speed of the rotor has the higher impact on energy consumption than for the gravel aggregates. Processing (comminution) of these aggregates requires more input of energy, probably due to the more rounded shape of single particles, causing it to be more difficult to disintegrate them in the crushing device. The width of gap has a much less significant impact on the energy consumption than speed of rotor and can be even disregarded in this approach.

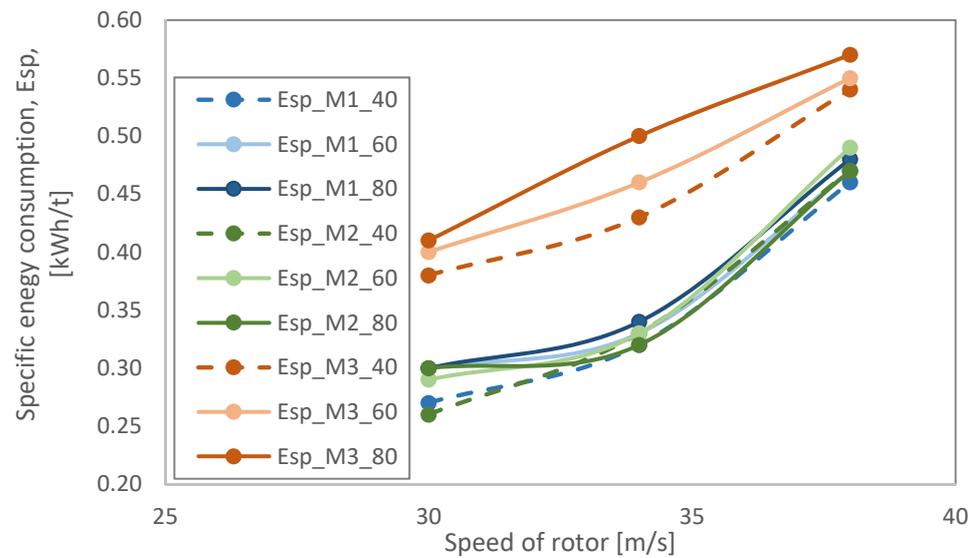


Figure 5. Energy consumption registered for various speeds of the rotor for materials M1–M3.

The yields of finest size fractions (i.e., below 2 mm) in individual crushing products are presented in Figure 6. The lowest content of fines was observed for the material M1, and equaled 11.72%, on average. For the limestone (M2), this value was nearly 2% higher (13.39%) and the highest value was observed for the gravel aggregate M3 and amounted to 14.97%. For the M2 and M3, a relationship between *FP1* and speed of rotor is inverse, while for the material M1 it is hard to determine a clear relationship, because depending on the gap width, the relationship is parabolic or inverse. The width of the gap, in turn, is proportional to the yield of finest products, regardless of the speed of the rotor (Figure 6).

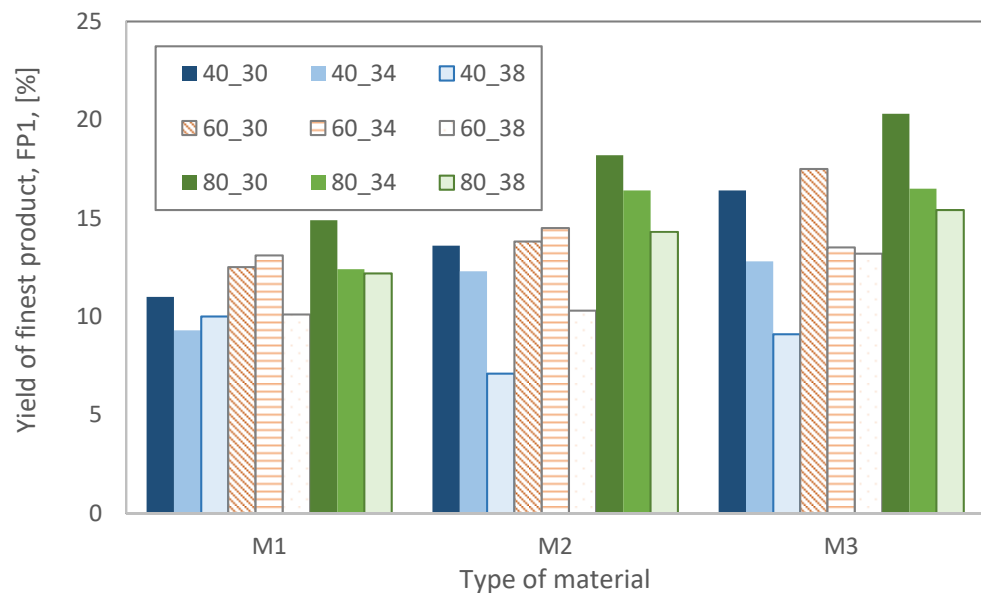


Figure 6. Yield of finest product obtained for respective setting of variables 1 and 2, materials M1–M3.

Analysis of values achieved for the 90% crushing ratio shows that the highest results were obtained for the width of gap 40 mm. Analogous values for the gaps of 60 and 40mm were significantly lower, regardless of the type of material. A significant impact of the speed of the rotor on the crushing ratio can be observed especially for M2 and M3, but mostly for the smallest gap. For 60 and 80 mm of gap values, there are rather insignificant variations observed in S_{90} values, both in terms of material type and the speed of the rotor (Figure 7).

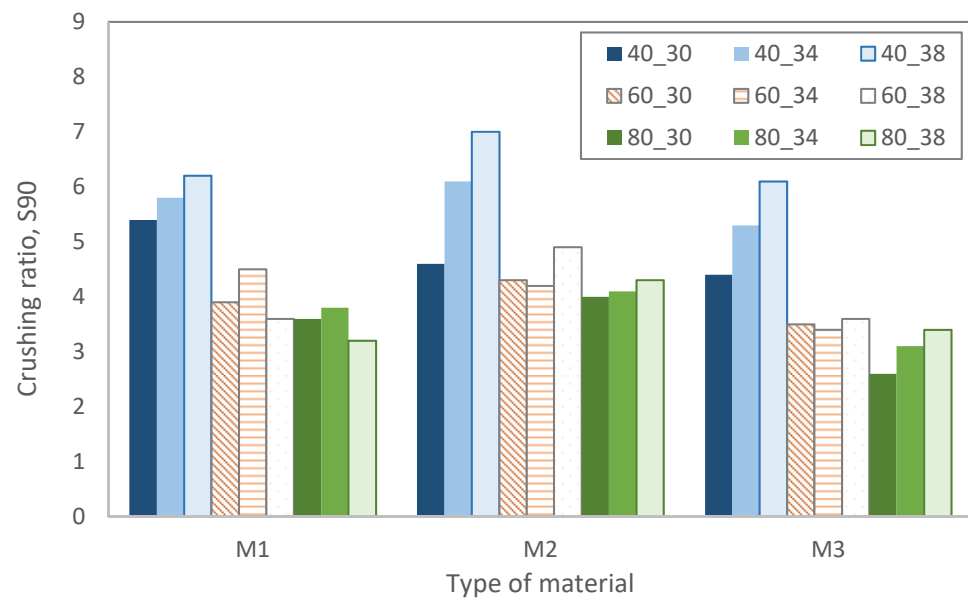


Figure 7. Size reduction ratio obtained for respective setting of variables 1 and 2, materials M1–M3.

In the second stage of experiments, two levels of values were accepted for analyzed variables. Results of investigations show that most achieved results (Figures 4 and 5) for the mid-values of speed of rotor and the gap are placed proportionally between the boundary values. Similar tendencies can be observed inspecting Figures 6 and 7. Therefore, only boundary values were taken into consideration in investigations, and for variable v_1 —speed of rotor—30 and 38 m/s were accepted, while for variable v_2 —the gap—40 and 80 mm widths were used. Two further materials, sandstone (M4) and diabase (M5), were tested and four tests in total were carried out for each material (see Table 1). The test results are presented in Tables 5 and 6.

Figure 8 presents relationships between the throughput speed of the rotor and the gap, while Figure 9 shows the correlation of the above variables with the specific energy consumption. Both relationships are similar in direction and changeability range to those established for materials M1–M3. For the limestone processing, a material comparably less resistant to comminution than the diabase, relatively higher throughput values and lower energy consumption were achieved. It is hard to decide definitely which of the variables has more significant impact on the throughput, but in the case of E_{sp} , the speed of the rotor has a slightly higher impact on energy consumption than the gap.

In the case of a yield of size fraction below 2 mm in crushing product, it can be seen that this content grows together with increasing the speed of the rotor. Lower contents of fines were achieved for the diabase for the gap width of 80 mm (Figure 10). For the size reduction ratio, in turn, the speed of rotor did not have a very significant impact, especially for the gap of 80 mm. On the other hand, a visible difference can be observed for products crushed at the gap of 40 mm, and a distinction regarding the type of material can be noticed for that value. For the gap of 80 mm, in turn, the achieved size reduction ratios are similar, regardless of the type of material (Figure 11).

Each product was also assessed in terms of the content of irregular particles. Yields of flat particles were determined using of a set of bar sieves, and values of flatness indices were obtained accordingly. For the material M1 the range of flatness index varied between 15 and 20%, for M2: 14–20%, for M3: 15–24%, for M4: 15–19%, and for M5: 19–22%. It can be seen that the most favorable results were achieved for materials M1 and M2, and the least favorable for the gravel (M3) and then diabase (M5). It is worth mentioning, however, that the lowest values of flatness index were achieved for the samples crushed at the highest speed of the rotor, regardless of the type of material.

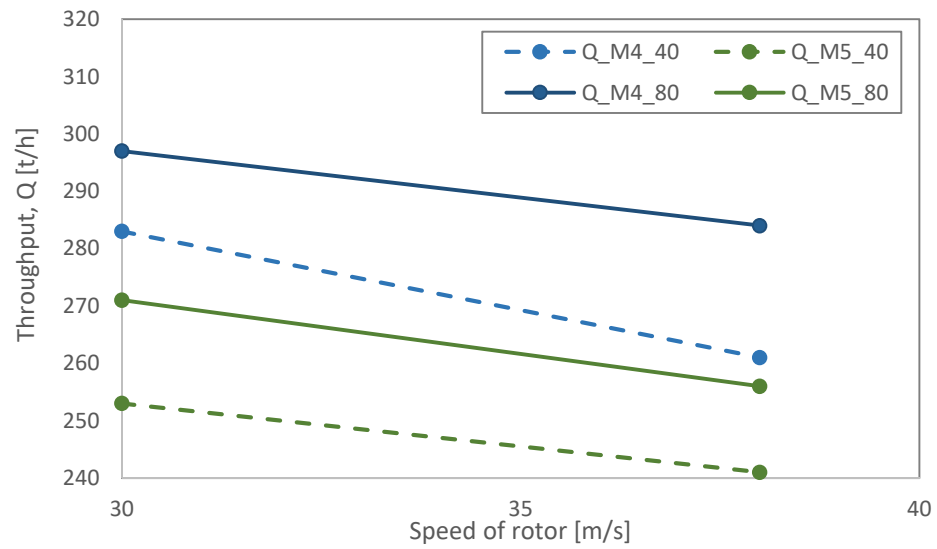


Figure 8. Results of throughput for various speeds of the rotor for materials M4 and M5.

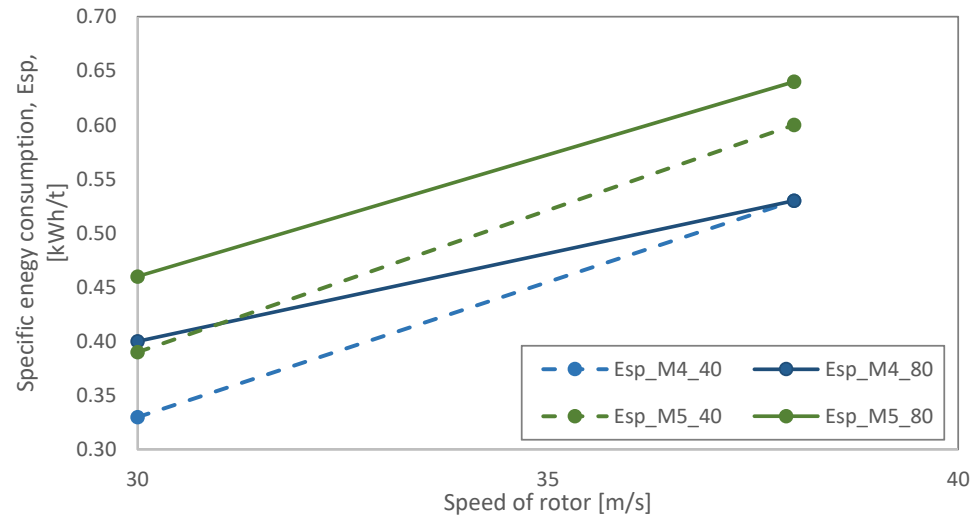


Figure 9. Energy consumption registered for various speeds of the rotor for materials M4 and M5.

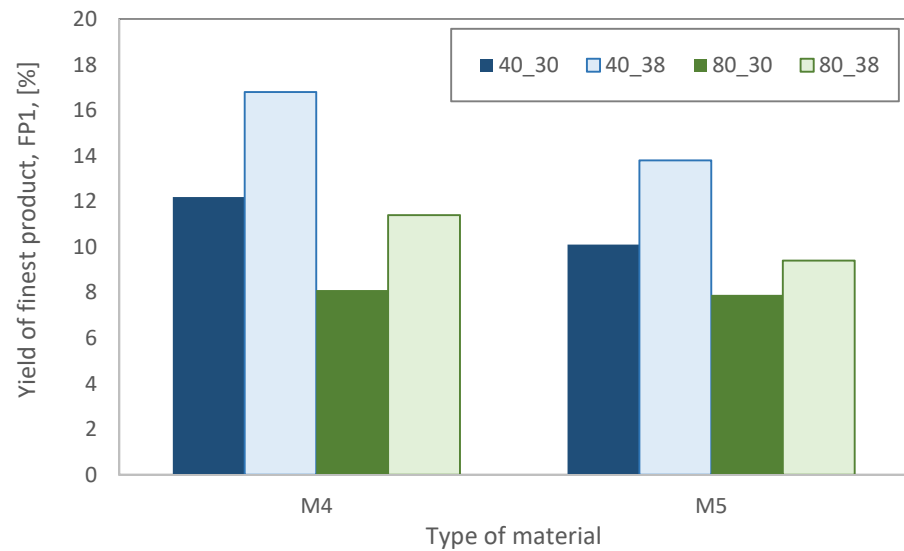


Figure 10. Yield of finest product obtained for respective setting of variables 1 and 2, materials M4 and M5.

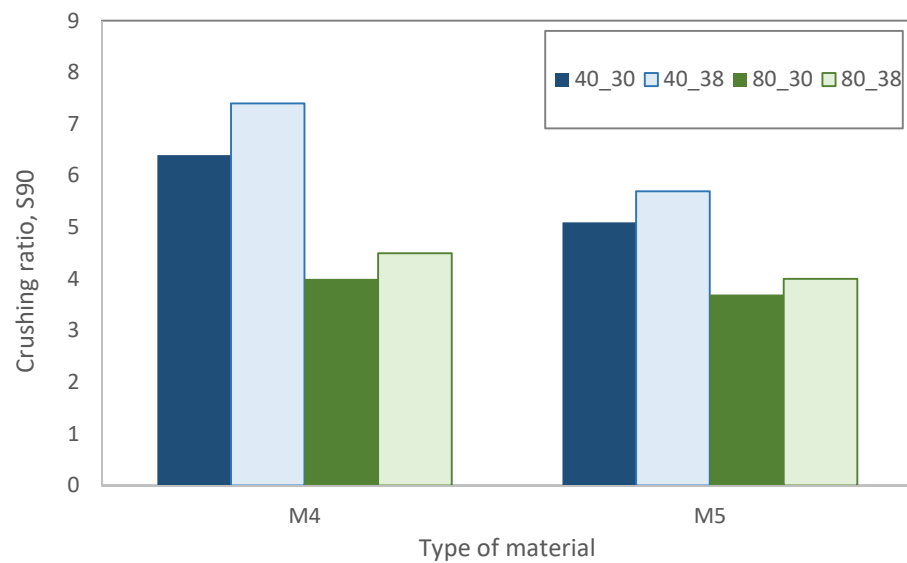


Figure 11. Size reduction ratio obtained for respective setting of variables 1 and 2, materials M4 and M5.

5. Analysis and Discussion

5.1. Modeling Results

The results of investigations were the starting point for building of general relationships describing the final product qualitative characteristics, in relation to operational parameters of the crusher device and process course. The models described the yield of the finest particles, i.e., below 2 mm (*FP1*), and 90% size reduction ratio (*S₉₀*). Significance of each independent variable in the model was checked at the significance level $1 - \alpha = 0.95$, and significant values were marked in red font. The model determination coefficient R^2 was also calculated for each model. Table 7 presents all models, calculated separately for each type of material, along with individual R^2 values.

Table 7. Models determined for each material.

Type of Material	Size Reduction Ratio, <i>S₉₀</i>		Yield of Finest Fractions, <i>FP1</i>	
	Model	R^2	Model	R^2
Dolomite	$S_{90} = 6.46 + 0.04v - 0.06e$	0.866	$FP1 = 1.74 + 0.38v - 0.05e$	0.803
Limestone	$S_{90} = 2.80 + 0.14v - 0.04e$	0.759	$FP1 = -2.19 + 0.66v - 0.12e$	0.877
Gravel	$S_{90} = 3.02 + 0.16v - 0.07e$	0.991	$FP1 = 0.99 + 0.58v - 0.10e$	0.979
Sandstone	$S_{90} = 6.36 + 0.09v - 0.07e$	0.992	$FP1 = 2.46 + 0.49v - 0.12e$	0.989
Diabase	$S_{90} = 5.04 + 0.06v - 0.04e$	0.988	$FP1 = 2.90 + 0.37v - 0.09e$	0.976

Results of modeling show that both models regarding the gravel material show full significances with all parameters. They are also characterized by very high levels of R^2 coefficients. In the case of dolomite and limestone, the models regarding the yield of finest size fractions (*FP1*) show full significance, but only the gap width appears to be significant in models for *S₉₀*. Values of R square are lower, comparing to the gravel. Models for the sandstone and diabase show values of R square even higher than in the case of analogous models for dolomite and limestone. However, both parameters appeared insignificant on the accepted level of significance $1 - \alpha$. Apart from the above differences, all models show the same direction in changeability of both parameters. Both types of models show an inverse relationship between dependent values and gap width *e*, while the relationship between speed of rotor and dependent values *S₉₀* and *FP1* is proportional.

In the second stage of modeling there were general models determined without distinguishing the type of material. Two technological parameters were added to the model, namely throughput *Q* and unit energy consumption *E_{sp}*—Formulas (5) and (6). The results of all experiments (in total 35 cases) were used for modeling.

$$FP1 = 8.64 + 0.66v - 0.07e - 0.04Q - 11.09Esp, R^2 = 0.805 \tag{5}$$

$$S_{90} = 1.89 + 0.07v - 0.06e + 0.01Q + 2.33Esp, R^2 = 0.825 \quad (6)$$

The results show that in the model describing the yield of the finest particle size fraction (*FPI*) all independent variables are statistically significant on confidence level $1 - \alpha = 0.95$. It shows that the variables were selected properly for the model, what is also in line with main assumptions and findings presented in [28]. Achieved values of model determination coefficients (R^2) confirm similar modeling results obtained for limestone [32]. In general, the gap width, throughput, and energy consumption have an inversely proportional effect on the value of γ . It means that in order to obtain the lowest possible yields of size fractions below 2 mm in the crushing product of an impactor, higher values of the outlet gap should be adopted. The process should be also carried out at higher throughput as well as higher linear velocity rotor. On the other hand, in the model characterizing the S_{90} size reduction ratio, only the gap width and throughput have a statistically significant impact on the dependent value—90% size reduction ratio.

5.2. Validation

The models presented in Section 5.1 show high level of determination, thus a high degree of explanation of the values of dependent variables through independent variables. All models are statistically significant at the probability level $1 - \alpha = 0.95$. The standard estimation error, SE, defined through Formula (7), was also calculated for each model from Table 8. The SE value determines average deviation of the model from empirical data.

$$SE = \sqrt{\frac{\sum_{i=1}^n (y_{emp} - \hat{y})^2}{n - 2}} \quad (7)$$

where y_{emp} —empirical results, obtained in the testing program or during verification; \hat{y} —modeling results. Table 8 contains values of SE, calculated for each type of material, separately for S_{90} and *FPI* models.

Table 8. Average values of SE calculated for each material and each type of model.

Type of Material	SE (S_{90})	SE (<i>FPI</i>)
Dolomite	0.51	0.85
Limestone	0.66	1.28
Gravel	0.68	1.21
Sandstone	2.18	0.55
Diabase	0.14	0.50

As can be seen from the table, the results indicate that content of the finest fractions (*FPI*) obtained from the model differs from empirical values from 0.5% to 1.28 %, while for size reduction ratio S_{90} from 0.14 to 2.18. The more favorable modeling results were achieved for models describing the finest fractions content in crushing products.

Apart from the SE calculations, a validation of models was performed. Fresh operating data on crushing the dolomite, limestone, and the gravel on plant scale was collected. Impact crusher was in operation at the speed of rotor 30 m/s and the calibrating gap width of 80 mm. Particle size distribution of the feed and crushing product for dolomite is presented in Figure 12 while more detailed results are included in Table 9.

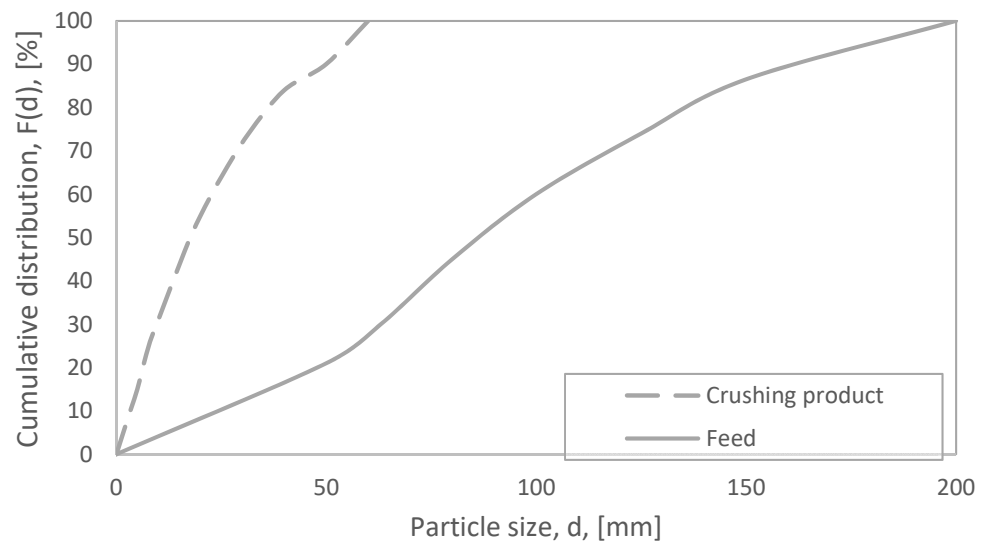


Figure 12. Particle size distribution of the feed and crushing product of dolomite.

Table 9. Values of SE for selected single test ($v = 30$ m/s, $e = 80$ mm), obtained for dolomite, limestone, and gravel.

Type of Material	Size Reduction Ratio, S_{90}		Yield of Finest Fractions, $FP1$	
	Empirical Value	Model	Empirical Value	Model
Dolomite	3.3	2.9	9.6	9.1
Limestone	4.3	3.8	9.4	8.0
Gravel	2.4	2.2	10.2	10.4

The presented results are generally in line with accuracy of specific models. The lowest differences between modeling and empirical results were achieved for the gravel (M3), and the models for this type of material were also characterized by highest values of R^2 . On the other hand, convergence of model and empiric situation for dolomite and limestone was also high, what, to some extent, confirms the proper selection of individual variables for the models and accepted modeling approach.

6. Summary and Conclusions

The results of the investigation presented in the paper showed that control of qualitative characteristics of the final aggregate products is to some extent possible through adjustment of a specific operation of the crushing device. It was also possible to design and build mathematical models of crusher operation, with independent variables connected to the feed characteristics and operational parameters of the machine.

Both obtained models i.e., describing the 90% size reduction ratio as well as characterizing the yield of finest particle size fraction, were convergent for each type of the tested material. However, the significance and influence of individual variables in models was diverse. The gap shows an inverse relationship with size reduction ratio and the yield of finest particle size fraction both in general models and in the models built separately for each type of feed material.

A very high level of model fitting was achieved, too. Only one model showed the value of determination coefficient R square lower than 80%. In six cases, the R^2 value was greater than 90%. Both general models achieved an R^2 value greater than 80%. Validation of the obtained model with real operational results for dolomite, limestone, and the gravel also show high degree of accuracy, especially for the latter material type. It proved that the modeling approach was selected properly, and that potential improvement of model accuracy can be achieved through more detailed investigative programs and additional independent variables can be investigated.

The presented models fit the specific situation, i.e., given technological circuit of aggregate production and individual type of crushing device. It is possible, however, to adopt this approach into different specifics of raw materials processing, provided certain assumptions and characteristics, related to such new operational practice, are implemented.

Author Contributions: Conceptualization, D.S.; methodology, T.G. and D.S. validation, D.S.; formal analysis, T.G. and D.S.; investigation, T.G.; data curation, D.S.; writing—original draft preparation, D.S. and T.G.; writing—review and editing, T.G. All authors have read and agreed to the published version of the manuscript.

Funding: This research received no external funding.

Acknowledgments: The article is the result of the National Center for Research and Development (NCBiR) project POIR.01.01.02-00-0014/16 “Przeprowadzenie prac rozwojowych w zakresie wytworzenia innowacyjnej linii demonstracyjnej do przeróbki surowców mineralnych”.

Conflicts of Interest: The authors declare no conflict of interest.

References

1. Naziemiec, Z. *Processing and Testing of Mineral Aggregates*; AGH Publishing House: Cracow, Poland, 2019. (In Polish)
2. Stempkowska, A.; Gawenda, T.; Naziemiec, Z.; Ostrowski, K.; Saramak, D.; Surowiak, A. Impact of the geometrical parameters of dolomite coarse aggregate on the thermal and mechanic properties of preplaced aggregate concrete. *Materials* **2020**, *13*, 4358. [[CrossRef](#)]
3. Rocco, C.; Elices, M. Effect of aggregate shape on the mechanical properties of a simple concrete. *Eng. Fract. Mech.* **2009**, *76*, 286–298. [[CrossRef](#)]
4. Mora, C.F.; Kwan, A.K.H. Sphericity, shape factor and convexity measurement of coarse aggregate for concrete using Digital image processing. *Cem. Concr. Res.* **2000**, *30*, 351–358. [[CrossRef](#)]
5. Cho, G.C.; Dodds, J.; Santamarina, J.C. Particle shape effects on packing density, stickness, and strength: Natural and crushed sands. *J. Geotech. Geoenviron. Eng.* **2006**, *132*, 591–602. [[CrossRef](#)]
6. Rouse, P.C.; Fannin, R.J.; Shuttle, D.A. Influence of roundness on the void ratio and strength of uniform sand. *Geotechnique* **2008**, *58*, 227–231. [[CrossRef](#)]
7. PN-EN 933-4:2008. Investigations on geometric properties of aggregates. Part 4. In *Determination of Particle Shape*; European Norm: Brussels, Belgium, 2008.
8. Kamani, M.; Ajalloeian, R. The effect of rock crusher and rock type on the aggregate shape. *Constr. Build. Mater.* **2020**, *230*, 117016. [[CrossRef](#)]
9. Naziemiec, Z.; Gawenda, T. Ocena efektów rozdrabniania surowców mineralnych w różnych urządzeniach kruszacych. *Pr. Nauk. Inst. Górnictwa Politech. Wrocławskiej. Konf.* **2006**, *115*, 83–94.
10. Gawenda, T. The influence of rock raw materials comminution in various crushers and crushing stages on the quality of mineral aggregates. *Miner. Res. Manag.* **2013**, *29*, 53–65. [[CrossRef](#)]
11. Malewski, J. Kształt ziaren w produktach kruszenia. *Kruszywa* **2014**, *3*, 52–55.
12. Gawenda, T. *Zasady Doboru Kruszarek Oraz Układów Technologicznych w Produkcji Kruszyw łamanych*. Monography no. 304; AGH Publishing House: Cracow, Poland, 2015.
13. Gawenda, T. Innovative technologies of the regular particle aggregates production. *Min. Sci.* **2015**, *22*, 45–59.
14. Gawenda, T.; Krawczykowski, D.; Krawczykowska, A.; Saramak, A.; Nad, A. Application of dynamic analysis methods into assessment of geometric properties of chalcedonite aggregates obtained by means of gravitational upgrading operations. *Minerals* **2020**, *10*, 180. [[CrossRef](#)]
15. Krawczykowski, D. Application of a vision systems for assessment of particle size and shape for mineral crushing products. *IOP Conf. Ser. Mater. Sci. Eng.* **2018**, *427*, 012013. [[CrossRef](#)]
16. Morrell, S. Predicting the overall specific energy requirement of crushing, high pressure grinding roll and tumbling mill circuits. *Min. Eng.* **2009**, *22*, 544–549. [[CrossRef](#)]
17. Tromans, D. Mineral comminution: Energy efficiency considerations. *Min. Eng.* **2008**, *21*, 613–620. [[CrossRef](#)]
18. Chakraborty, M.K.; Ahmad, M.; Singh, R.S.; Pal, D.; Bandopadhyay, C. Determination of the emission rate from various opencast mining operations. *Environ. Model. Softw.* **2002**, *17*, 467–480. [[CrossRef](#)]
19. Saramak, A.; Naziemiec, Z. Determination of dust emission level for various crushing devices. *Min. Sci.* **2019**, *26*, 45–54. [[CrossRef](#)]
20. Saramak, A. Comparative Analysis of Selected Types of Crushing Forces in Terms of Dust Emission. *Inżynieria Miner. -J. Pol. Miner. Eng. Soc.* **2019**, *2*, 151–154.
21. Saramak, A.; Naziemiec, Z.; Saramak, D. Analysis of noise emission for selected crushing devices. *Min. Sci.* **2016**, *23*, 145–154. [[CrossRef](#)]

22. Hubbard, S.J. *Evaluation of Fugitive Dust Emissions from Mining—Report*; PEDCo-Environmental Specialists Inc.: Cincinnati, OH, USA, 1976.
23. Huertas, J.; Camacho, D.; Huertas, M. Standardized emissions inventory methodology for open pit mining areas. *Environ. Sci. Pollut. Res.* **2012**, *19*, 2784–2794. [[CrossRef](#)]
24. Tian, S.; Liang, T.; Li, K. Fine road dust contamination in a mining area presents a likely air pollution hotspot and threat to human health. *Environ. Intern.* **2019**, *128*, 201–209. [[CrossRef](#)]
25. Zhou, C.; Zhang, M.; Li, Y.; Lu, Y.; Chen, J. Influence of particle shape on aggregate mixture's performance: DEM results. *Road Mater. Pavement Des.* **2019**, *20*, 399–413. [[CrossRef](#)]
26. Jamkar, S.S.; Rao, C.B. Index of Aggregate Particle Shape and Texture of coarse aggregate as a parameter for concrete mix proportioning. *Cem. Concr. Res.* **2004**, *34*, 2021–2027. [[CrossRef](#)]
27. Umucu, Y.; Deniz, V.; Cayirli, S. A New Model for Comminution Behavior of Different Coals in an Impact Crusher. *Energy Sources Part A Recovery Utiliz. Environ. Eff.* **2014**, *36*, 1406–1413. [[CrossRef](#)]
28. Bearman, R.A.; Briggs, C.A. The active use of crushers to control product requirements. *Min. Eng.* **1998**, *11*, 849–859. [[CrossRef](#)]
29. Whiten, W.J. A model for simulating crushing plants. *J. S. Afr. Inst. Min. Met.* **1972**, *72*, 257.
30. Whiten, W.J.; White, M.E. Modeling and simulation of high tonnage crushing plants. In Proceedings of the 12th International Mineral Processing Congress, Sao Paulo, Brazil, 22–26 September 1975; 2, pp. 148–158.
31. Nikolov, S. A performance model for impact crushers. *Min. Eng.* **2002**, *15*, 715–721. [[CrossRef](#)]
32. Deniz, V. A new size distribution model by t-family curves for comminution of limestones in an impact crusher. *Adv. Powder Technol.* **2011**, *22*, 761–765. [[CrossRef](#)]
33. Umucu, Y.; Deniz, V.; Unal, N. An evaluation of a modified product size distribution model based on t-family curves for three different crushers. *Physicochem. Probl. Min. Proc.* **2013**, *49*, 473–480.
34. Tumidajski, T.; Saramak, D. *Methods and Models of Mathematical Statistics in Mineral Processing*; AGH Publishing House: Cracow, Poland, 2009; pp. 1–304.
35. Saramak, D.; Lagowski, J.; Gawenda, T.; Saramak, A.; Stempkowska, A.; Foszcz, D.; Lubieniecki, T.; Lesniak, K. Modeling of washing effectiveness in a high-pressure washing device obtained for crushed-stone and gravel aggregates. *Resources* **2020**, *9*, 119. [[CrossRef](#)]